applied sciences

MDPI

Article

Adsorption of CO_2 on ZSM-5 Zeolite: Analytical Investigation via a Multilayer Statistical Physics Model

Fatma Aouaini [1,*], Nadia Bouaziz [2], Wafa Alfwzan [3], Noura Khemiri [4], Zainab Elqahtani [1] and Abdelmottaleb Ben Lamine [2]

[1] Department of Physics, College of Science, Princess Nourah bint Abdulrahman University, P.O. Box 84428, Riyadh 11671, Saudi Arabia; zainebqahtani@pnu.edu.sa
[2] Laboratory of Quantum and Statistical Physics, LR18ES18, Faculty of Sciences of Monastir, Monastir University, Monastir 5000, Tunisia; nadiabouaziz22@yahoo.fr (N.B.); abdelmottaleb.benlamine@fsm.rnu.tn (A.B.L.)
[3] Mathematical Sciences Department, College of Science, Princess Nourah bint Abdulrahman University, P.O. Box 84428, Riyadh 11671, Saudi Arabia; wfalfwzan@pnu.edu.sa
[4] Department of Physics, College of Sciences at Yanbu, Taibah University, Yanbu, Medina 42353, Saudi Arabia; Khemiri.noura58@gmail.com
* Correspondence: fasaidi@pnu.edu.sa

Abstract: In this paper, a synthesized zeolite (ZSM-5) is used as an adsorbent to analyze the adsorption phenomenon of carbon dioxide. This investigation, based on the statistical physics treatment, applied the multilayer model with saturation to understand the CO_2 adsorption on four samples, namely M-ZSM-5 (M = Na^+, Mg^{2+}, Zn^{2+}, La^{3+}), at various temperatures T = 0 °C, 30 °C and 60 °C. The modeling results indicated that CO_2 adsorption occurred via a non-parallel orientation on the ZSM-5 surface. The CO_2 adsorption capacities varied from 26.14 to 28.65 cm^3/g for Na-ZSM-5, from 25.82 to 27.97 cm^3/g for Mg-ZSM-5, from 54.82 to 68.63 cm^3/g for La-ZSM-5 and from 56.53 to 74.72 cm^3/g for Zn-ZSM-5. Thus, Zn-ZSM-5 exhibits the highest adsorption amount. The analysis of the adsorption energies shows that the adsorption of CO_2 on ZSM-5 zeolite is a physisorption phenomenon that could be controlled thanks to the energy parameters obtained via the numerical findings using the multilayer statistical model. Finally, the distribution of site energy was determined to confirm the physical character of the interactions between adsorbate/adsorbent and the heterogeneity of the zeolite surface.

Keywords: CO_2 adsorption; ZSM-5; multilayer model; statistical physics

Citation: Aouaini, F.; Bouaziz, N.; Alfwzan, W.; Khemiri, N.; Elqahtani, Z.; Lamine, A.B. Adsorption of CO_2 on ZSM-5 Zeolite: Analytical Investigation via a Multilayer Statistical Physics Model. *Appl. Sci.* **2022**, *12*, 1558. https://doi.org/10.3390/app12031558

Academic Editor: Joana F. B. Barata

Received: 20 December 2021
Accepted: 27 January 2022
Published: 31 January 2022

1. Introduction

Human activities, particularly the combustion of natural gas and fossil fuels, are regarded as the main causes of global warming and accordingly the increment of carbon dioxide (CO_2) emissions in the air [1–3]. Reducing the concentration of this gas before it is transmitted into the air is an urgent issue and has become an important challenge for the scientific community to safeguard the planet's environment. Carbon capture and storage (CCS) technology is regarded as a promising mechanism for the beneficial CO_2 concentration reduction in the atmosphere [4]. Cryogenic separation mechanisms [5], membrane-based processes [6], solid adsorbents adsorption [7] and aqueous amine absorption [8] are also carbon capture technologies that require even more research to remedy the shortcomings of the present step. Especially the synthesis of adsorbents, which must be cheap and appropriate for industrial conditions, and flue gas are main research questions. A broad choice of porous adsorbents is available for usage in pressure/temperature swing adsorption to segregate carbon dioxide from industrial flue gas, such as hydrotalcite [9], zeolites [10–12], mesoporous silica [13] and activated carbon [14]. Zeolite is a pore-plentiful solid adsorbent with an electric field region because of their intrinsically

negatively charged cations and their frameworks presenting important physical characteristics [15]. As a zeolite adsorbent, greatly crystalline ZSM-5 presents a great chemical/thermal stability and an elevated surface area and thereby is frequently utilized in the domain of gas separation and catalysis [16–19]. The use of extra-framework cations in the zeolite equilibrates the negative charge in the silica-alumina framework; the various kinds of cations will also modify the electrostatic field, the structure of the internal pore and the crystallinity [20–22]. Moreover, these cations can ameliorate the application performance and depict a great effect on the physicochemical properties; however, concerning the CO_2 adsorption performance, the impacts of different cations outside the zeolite framework have been insufficiently investigated.

It is noteworthy that the theoretical and experimental studies of the adsorption process on ZSM-5 zeolite are pertinent research topics with the object of ameliorating the CO_2 adsorption phenomenon related to these compounds. Particularly, the modeling utilizing the statistical physics can describe well the adsorption of carbon dioxide on ZSM-5 zeolites. For this study, the analysis of the adsorption process using the analytical model depended on the explanation of the energetic and steric parameters of the CO_2 adsorption for many adsorbents [23,24].

In this work, the impact of extra-framework cation in ion-exchanged ZSM-5 is analyzed and interpreted utilizing statistical physics formalism. Experimental isotherms are employed to determine the statistical physics parameters to study the CO_2 adsorption on this zeolite. Statistical simulation also makes it possible to analyze the interactions between the CO_2 gas and the zeolite surface and to estimate the corresponding energies.

2. Experimental Section

The adsorption isotherms of CO_2 on M-ZSM-5 (M = Na^+, Mg^{2+}, Zn^{2+}, La^{3+}) were measured experimentally and employed to apply the models of the statistical physics approach, for the interpretation of the corresponding phenomenon. The ZSM-5 zeolites, obtained by the hydrothermal synthesis technique [25], were amended by cation exchange using the impregnation way with different metal ion solutions. The final samples used as adsorbent were named M-ZSM-5, depending on the cation kind (M = Mg^{2+}, La^{3+}, Zn^{2+}, Na^+). A total of 200 mg of each tested zeolite was utilized to determine CO_2 adsorption isotherms at three temperatures (0 °C, 30 °C and 60 °C) on a JWBK112 volumetric adsorption analyzer. The control of this step is achieved through constant temperature water or ice water mixture. To remove moisture and impure gases before the measurement, the substance was heated under vacuum for 5 h at 350 °C after placing it in a glass tube [25]. The purity of the CO_2 gas utilized in the adsorption experiment was 99.999%.

3. Modeling Analysis

Adsorption isotherms are the result of interactions between the adsorbate (CO_2 gas) and the sample surface (M-ZSM-5). The interpretation of the experimental isotherms represents an important step in interpreting the adsorption phenomenon. In addition to the experimental results, all the measured isotherms were examined and comprehended through modeling using the statistical physics theory according to the grand canonical ensemble. Consequently, three physical models were selected to fit the measured data.

3.1. Monolayer Model with One Energy (M1)

The first model supposed that the CO_2 adsorption on ZSM-5 zeolites took place by the creation of a single layer (Figure 1). The interactions between CO_2 molecules with M-ZSM-5 adsorbents are described by a specified energy ($-\varepsilon$), which is the same for all the binding sites involved in CO_2 adsorption. The expression of the model is given by the relation as follows [26]:

$$Q_a = nD_0 = \frac{nD_m}{1 + \left(\frac{P_{1/2}}{P}\right)^n} \quad (1)$$

Figure 1. Schematic illustration of the distribution of the molecules adsorbed on a solid according to the monolayer model with a single energy.

The parameter n defines the number of CO_2 molecules captured by the sites of the ZSM-5 sample; $P_{1/2}$ defines the half saturation pressure of the created layer; and D_m is the density of active sites of the tested samples.

3.2. Monolayer Model with Two Energies (M2)

For this model, we supposed that the creation of two layers was described via two adsorption energies $(-\varepsilon_1)$ and $(-\varepsilon_2)$ (Figure 2). These energies define the interactions between the CO_2 molecules and between the CO_2 and ZSM-5 surface. This model is given by the relationship as follows [26]:

$$Q_a = nD_m \frac{\left(\frac{P}{P_1}\right)^n + 2\left(\frac{P}{P_2}\right)^{2n}}{1 + \left(\frac{P}{P_1}\right)^n + \left(\frac{P}{P_2}\right)^{2n}} \quad (2)$$

where P_1 and P_2 are the pressures at half-saturation relating, respectively, to the first and second layers.

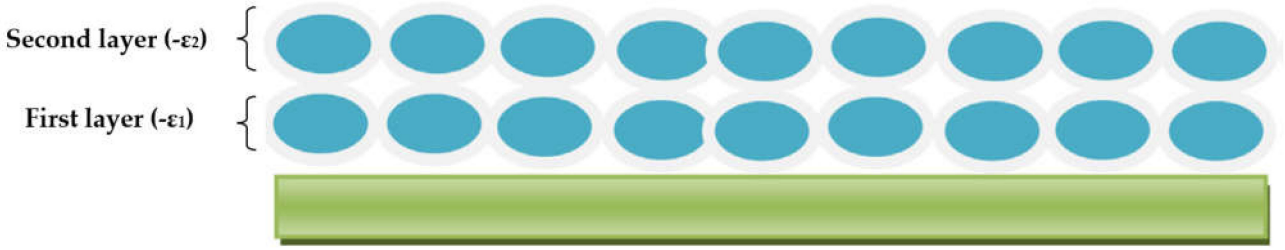

Figure 2. Schematic illustration of the distribution of the molecules adsorbed on a solid according to the double layer model with two energies.

3.3. Multilayer Model (M3)

In this case, the adsorption of CO_2 on ZSM-5 zeolite was carried out by the formation of various adsorption layers (Figure 3). Thus, the first adsorbed layer that can be formed directly with the surface of ZSM-5 was effectuated with a first adsorption energy, and the additional layers related to CO_2–CO_2 interaction required a second interaction energy. Therefore, the entire number of adsorption layers is $N_c = 1 + N_2$. The analytical equation of the multilayer model has the following form [26]:

$$Q_a = n.D_m.\frac{\frac{-2\left(\frac{P}{P_1}\right)^{2n}}{\left(1-\left(\frac{P}{P_1}\right)^n\right)} + \frac{\left(\frac{P}{P_1}\right)^n\left(1-\left(\frac{P}{P_1}\right)^{2n}\right)}{\left(1-\left(\frac{P}{P_1}\right)^n\right)^2} + 2\frac{\left(\frac{P}{P_1}\right)^n\left(\frac{P}{P_2}\right)^n\left(1-\left(\frac{P}{P_2}\right)^{nN_2}\right)}{\left(1-\left(\frac{P}{P_2}\right)^n\right)} - \frac{\left(\frac{P}{P_1}\right)^n\left(\frac{P}{P_2}\right)^n\left(\frac{P}{P_2}\right)^{nN_2}N_2\left(1-\left(\frac{P}{P_2}\right)^n\right)}{\left(1-\left(\frac{P}{P_2}\right)^n\right)} + \frac{\left(\frac{P}{P_1}\right)^n\left(\frac{P}{P_2}\right)^{2n}\left(1-\left(\frac{P}{P_2}\right)^{nN_2}\right)}{\left(1-\left(\frac{P}{P_2}\right)^n\right)^2}}{\frac{\left(1-\left(\frac{P}{P_1}\right)^{2n}\right)}{\left(1-\left(\frac{P}{P_1}\right)^n\right)} + \frac{\left(\frac{P}{P_1}\right)^n\left(\frac{P}{P_2}\right)^n\left(1-\left(\frac{P}{P_2}\right)^{nN_2}\right)}{\left(1-\left(\frac{P}{P_2}\right)^n\right)}} \quad (3)$$

where P_1 and P_2 are the pressures at half saturation corresponding, respectively, to the first and to the $1+N_2$ layers.

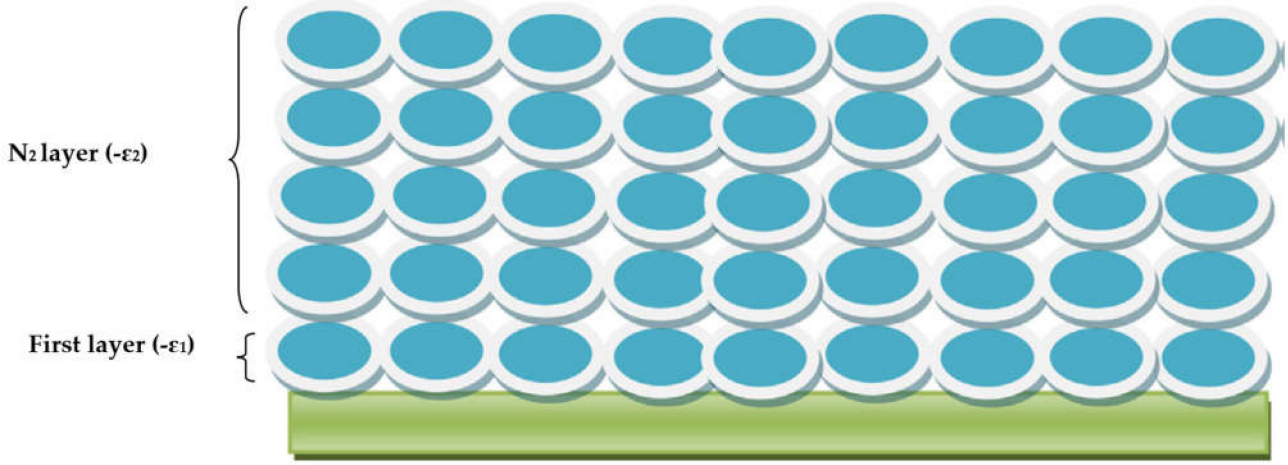

Figure 3. Schematic illustration of the distribution of the molecules adsorbed on a solid according to the multilayer model with saturation.

4. Advanced Modeling Analysis

All measured isotherms were fitted using three analytical models. Indeed, the adjusting findings show that the parameters of the monolayer model were not acceptable to supply a reasonable investigation of the CO_2 adsorption process. By way of example, the capacity values of CO_2 adsorption at certain temperature are not compatible with the experimental findings. This model is therefore inappropriate to investigate the CO_2 adsorption phenomenon. Concerning the double-layer model, we can notice that the temperature impact on the fitted parameters is not comprehensible and the model is also rejected. For the multilayer model, their parameters are very reasonable and the effect of the temperature on them is evident, in addition to the correlation coefficients R^2, which are very close to unity (from 0.997 to 0.999) (Table 1). Consequently, the multilayer model is chosen to analyze the CO_2 adsorption process on the ZSM-5 zeolite. The parameter values of the chosen model are listed in Table 2. These values are determined by a numerical simulation utilizing the Levenberg–Marquardt algorithm and a multivariable non-linear regression. Figure 4 depicts the adsorption isotherms fitted by the multilayer model.

Table 1. Values of adjustment coefficient R^2 for the three models.

Adsorbents	Temperature (K)	Coefficient of Determination R^2		
		M1	M2	M3
Na-ZSM-5	0 °C	0.896	0.969	**0.997**
	30 °C	0.861	0.970	**0.999**
	60 °C	0.921	0.985	**0.999**
Mg-ZSM-5	0 °C	0.713	0.951	**0.999**
	30 °C	0.689	0.902	**0.998**
	60 °C	0.741	0.981	**0.998**
La-ZSM-5	0 °C	0.762	0.920	**0.999**
	30 °C	0.802	0.911	**0.997**
	60 °C	0.831	0.899	**0.997**
Zn-ZSM-5	0 °C	0.812	0.931	**0.999**
	30 °C	0.791	0.962	**0.999**
	60 °C	0.851	0.973	**0.999**

Table 2. Values of the different adjusted parameters according to the multilayer model with saturation (M3).

Adsorbents	Temperature (K)	Parameters					
		n	D_m	N_c	Q_{sat}	$(-\varepsilon_1)$	$(-\varepsilon_2)$
Na-ZSM-5	0 °C	3.23	11.83	1.75	28.65	−15.265	−10.702
	30 °C	2.55	10.72	2.02	27.88	−17.022	−11.87
	60 °C	2.39	9.27	2.18	26.14	−18.772	−13.244
Mg-ZSM-5	0 °C	1.44	16.75	2.16	27.97	−16.696	−10.491
	30 °C	1.02	13.92	2.89	26.83	−17.543	−10.561
	60 °C	0.99	13.31	2.94	25.82	−19.27	−11.989
La-ZSM-5	0 °C	0.85	42.95	2.88	68.63	−17.426	−9.15
	30 °C	0.81	33.32	3.23	60.18	−18.271	−10.441
	60 °C	0.79	30.56	3.43	54.82	−19.154	−11.833
Zn-ZSM-5	0 °C	1.51	40.9	2.21	74.72	−16.061	−10.4
	30 °C	1.05	34.2	2.7	61.74	−16.748	−10.761
	60 °C	1.01	25.31	3.19	56.53	−18.628	−11.468

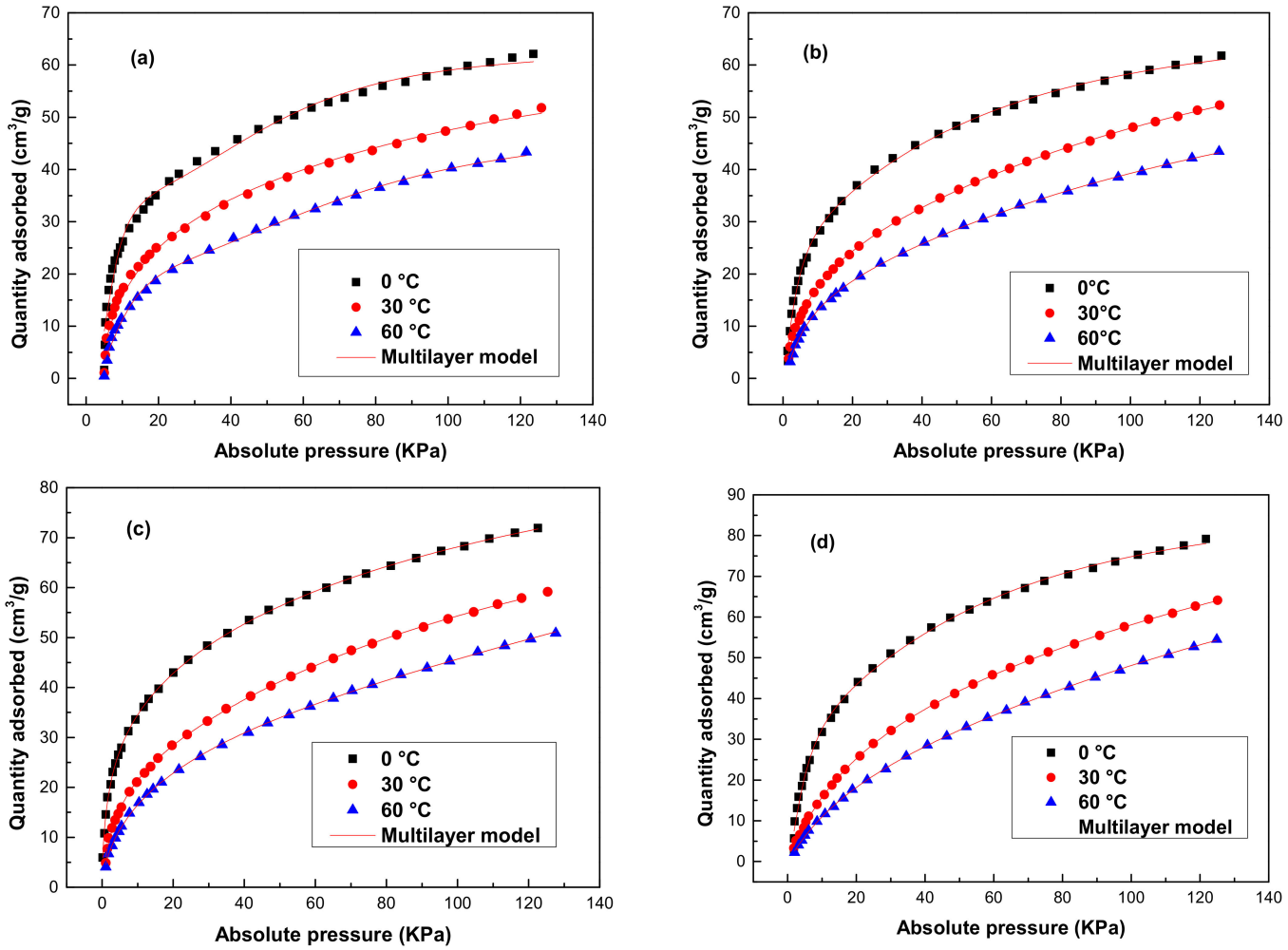

Figure 4. Experimental adsorption isotherms of CO_2 on (**a**) Na-ZSM-5, (**b**) Mg-ZSM-5, (**c**) La-ZSM-5 and (**d**) Zn-ZSM-5 at three temperature and fitting by multilayer statistical physics model (M3).

5. Analysis of the Steric Parameters

5.1. Number of Molecules Adsorbed per Captured Site (n)

The parameter n provides significant details regarding the adsorption of CO_2 on ZSM-5. In particular, this parameter is employed to determine the adsorption position of CO_2 molecules on the surface of ZSM-5 and their degree of aggregation. Previous research has revealed that three possibilities can take place to analyze the adsorption position according to the 'n' values [27,28]:

Possibility 1: if $n < 0.5$, for this condition, the receptor site adsorb a portion of a molecule per site defining a parallel adsorption orientation and consequently a multi-linking adsorption mechanism.

Possibility 2: if $0.5 < n < 1$, this case assumes that the CO_2 molecules are accepted through a non-parallel and parallel orientation with two various percentages at the same time.

Possibility 3: if $n \geq 1$, the active site accepts one or more CO_2 molecules showing that the position of adsorption is non-parallel, which reveals a multi-molecular adsorption phenomenon.

According to the values of this parameter, as depicted in Table 2, the values of n for the La-ZSM-5 system are 0.85, 0.81 and 0.79, respectively, at 0, 30, and 60 °C. These values indicate that the CO_2 molecules are adsorbed via a mixed adsorption orientation (i.e., non-parallel and parallel at the same time). For the Na-ZSM-5, Mg-ZSM-5 and Zn-ZSM-5 systems, all values of n are higher than one (multi-molecular adsorption process), showing that the adsorption of CO_2 molecules takes place through a non-parallel orientation. For instance, the value of n is 2.39 during the CO_2 adsorption on Na-ZSM-5 at 60 °C. This value is analyzed with the following equation: $2.39 = 2.x + (1\text{-}x) \times 3$, where x depicts the sites occupied by two molecules and 1-x represents the sites occupied by three CO_2 molecules. This calculation reveals that 61% of the sites are occupied by two molecules of CO_2, while 39% are occupied by three molecules. Figure 5 illustrates the relationship between n and the tested temperature. We are observed the decrease in the number of docked molecules per site with the temperature since it varies from 2.39 to 3.23, from 0.99 to 1.44, from 0.79 to 0.85, and from 1.01 to 1.51, respectively, for CO_2-Na-ZSM-5, CO_2-Mg-ZSM-5, CO_2-La-ZSM-5, and CO_2-Zn-ZSM-5. Thus, we can conclude that the adsorption systems are thermally deactivated and the temperature presents a negative impact (i.e., decrease inn) on the aggregation phenomenon.

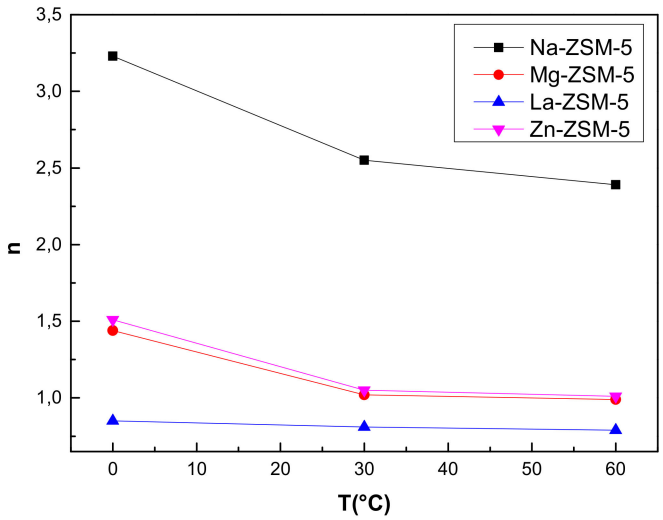

Figure 5. Effect of temperature on the number of CO_2 molecules captured on the Na-ZSM-5, Mg-ZSM-5, La-ZSM-5 and Zn-ZSM-5 adsorbents.

The comparison of the numbers of adsorbed molecules per site for all tested samples at all operating temperatures indicates that $n(La^{3+}) < n(Mg^{2+}) < n(Zn^{2+}) < n(Na^{+})$. We can explain this behavior by the affinity of each adsorbent and the difference of porosity.

5.2. Density of Binding Sites (D_m)

The effect of temperatures on parameter D_m is depicted in Figure 6. This coefficient represents the effectively density per surface unit of occupied receptor sites. Evidently, the rise in temperature leads to a decrease in the density of the host sites for all the samples. Overall, this decrease is clarified by the thermal agitation. Indeed, the increment in temperature causes the blockage of binding sites on the ZSM-5 surface, which can intervene in the adsorption mechanism and have negative effects on the performance of the adsorbents. We have remarked that the receptor site densities of La-ZSM-5 and Zn-ZSM-5 are evidently greater than the receptor site densities of Mg-ZSM-5 and Na-ZSM-5. This is due firstly to the existence of RE element oxides (ZnO_2 and LaO_2) in the structure of zeolite, enhancing the field of internal electrostatic and therefore the activation of the zeolite surface, which improves the CO_2 adsorption [29,30]. Then, the formed aggregate size is greater in Na-ZSM-5, which prevents the activation of the zeolite surface.

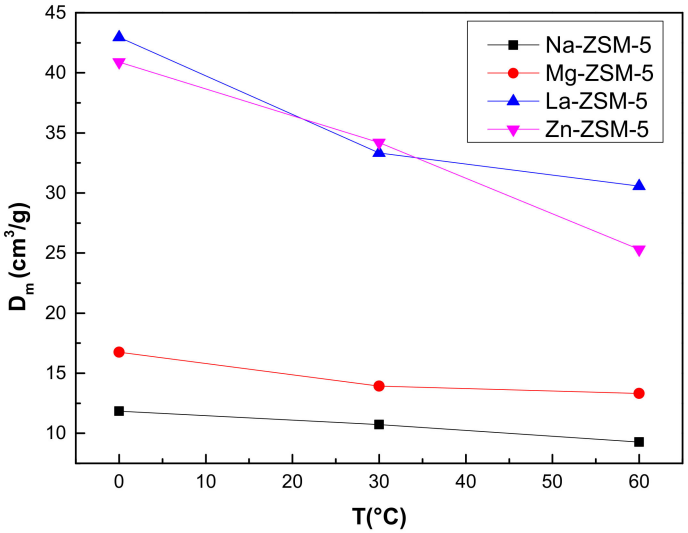

Figure 6. Effect of temperature on the density of receptor sites of the Na-ZSM-5, Mg-ZSM-5, La-ZSM-5 and Zn-ZSM-5adsorbents.

5.3. Total Number of Adsorbed Layers (N_c)

The parameter $N_c = 1+N_2$ defines the entire number of formed layers established during the adsorption process. The estimated number of the total CO_2 created layers of the four adsorbents ranged from 2.02 to 3.43. According to this result, we found that CO_2 adsorption is almost realized by the creation of approximately two or three adsorbed layers according to the tested temperature. The relationship between the temperature and the global number of layers (Figure 7) shows the increment in this parameter with the adsorption temperatures, which may be the consequence of weak interaction energies. The N_c values are non-integer, which shows that the layers are at time incomplete in the adsorption phenomenon.

5.4. Adsorption Quantity at Saturation (Qsat)

The potentiality of the surface to capture CO_2 molecules from the four samples is illustrated by the saturated adsorption capacity Q_{sat}. This means that this parameter is presented as the highest amount that can be captured at each temperature. Using the appropriate model, this parameter is expressed by:

$$Q_{sat} = n \times D_m \times N_c \quad (4)$$

The temperature impact on the adsorption amount at saturation is given in Figure 8. We noticed that the increase in temperature provokes the decrement inQ_{sat} for all the

systems, which is attributed to the exothermic character of the adsorption mechanism and to the temperature impact on the aggregation phenomenon. The decrease in the saturated adsorption quantity is the result of the reduction in the force of the relation between the ZSM-5 surface and CO_2 molecules.

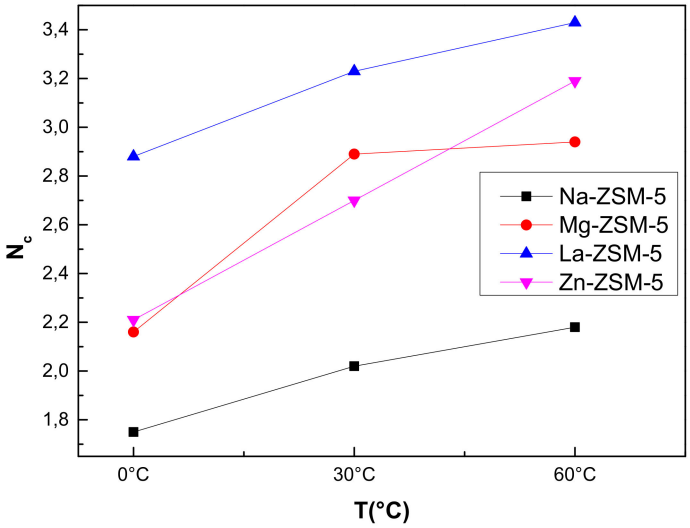

Figure 7. Effect of temperature on the total number of formed layers of CO_2 molecules on the Na-ZSM-5, Mg-ZSM-5, La-ZSM-5 and Zn-ZSM-5 adsorbents.

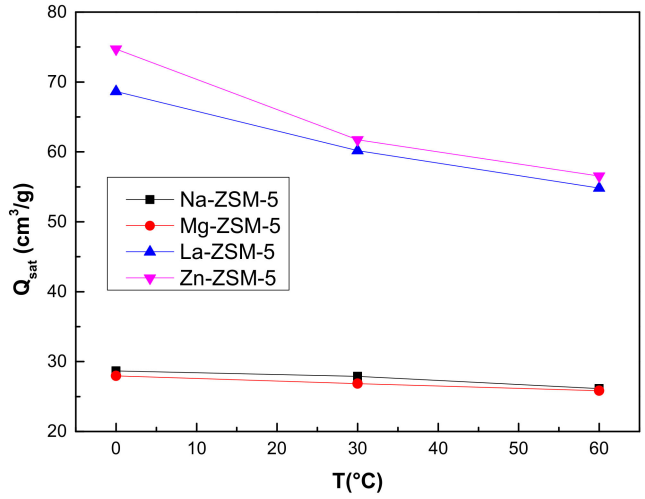

Figure 8. Effect of temperature on CO_2 adsorption capacity at saturation for the Na-ZSM-5, Mg-ZSM-5, La-ZSM-5 and Zn-ZSM-5adsorbents.

The CO_2 adsorption capacity decreased with the order of Zn-ZSM-5 > La-ZSM-5 > Na-ZSM-5 > Mg-ZSM-5 at the three temperatures, whereas the size of the tested metal cation radius decreased in the order of La^{3+} (0.1032 nm) > Na^{+} (0.102 nm) > Zn^{2+} (0.074 nm) > Mg^{2+} (0.072 nm). In addition to the charge and size of the extra-framework cations, which are reflected on the CO_2 adsorption quantity, the kind of cation, the density and position in the structure of zeolite framework also have a strong effect. The low adsorption capacity of Mg-ZSM-5 is ascribed to the weak affinity of the alkaline earth metal cations for CO_2, which is consistent with the behavior related to alkaline earth metal cation-exchanged zeolite beta [31]. The Zn^{2+} cation of the transition metal group has little cation radius and is favorably situated at the site of IV leads to an important increment in adsorption performance, which was revealed by the same manner for the ZnCHA [32–34].

6. Interpretation of the Adsorption Energy

The multilayer model supplied two energies ($-\varepsilon_1$) and ($-\varepsilon_2$) during the adsorption process, which are utilized to describe the kind of interactions between the CO_2 molecules and also between the zeolite surface and the CO_2 molecules. The two energies are determined by the next expressions [34–36]:

$$-\varepsilon_1 = -\mathrm{RTLn}\frac{P_{vs}}{P_1} \quad (5)$$

$$-\varepsilon_2 = -\mathrm{RTLn}\frac{P_{vs}}{P_2} \quad (6)$$

where P_{vs} represents the vapor pressure at saturation of CO_2.

The adsorption energies are determined based on the pressures at half-saturation (P_1 and P_2) evaluated by model application. These pressures are principally related to the first layers and those created by N_2 during the adsorption mechanism. The values of the determined energies listed in Table 2 are inferior to 30 kJ/mol, indicating that the CO_2 adsorption on ZSM-5 can be related to a physisorption phenomenon for which the van der Waals interactions are responsible. In addition, the values of the adsorption energies are negative confirming the exothermic nature of the CO_2 adsorption on the tested samples.

The temperature effect on the adsorption energies are illustrated in Figure 9. It is evident that the adsorption energies reduce with temperature, which is clarified by the decrement in the accessible binding sites and consequently the decrement in the average active site energy [37]. In fact, the molecules of carbon dioxide are initially bonded on the sites presenting intense affinity with a high adsorption energy. After the occupation of these sites, the molecules of carbon dioxide are bonded through sites characterized by lower adsorption energy that is actually decreased.

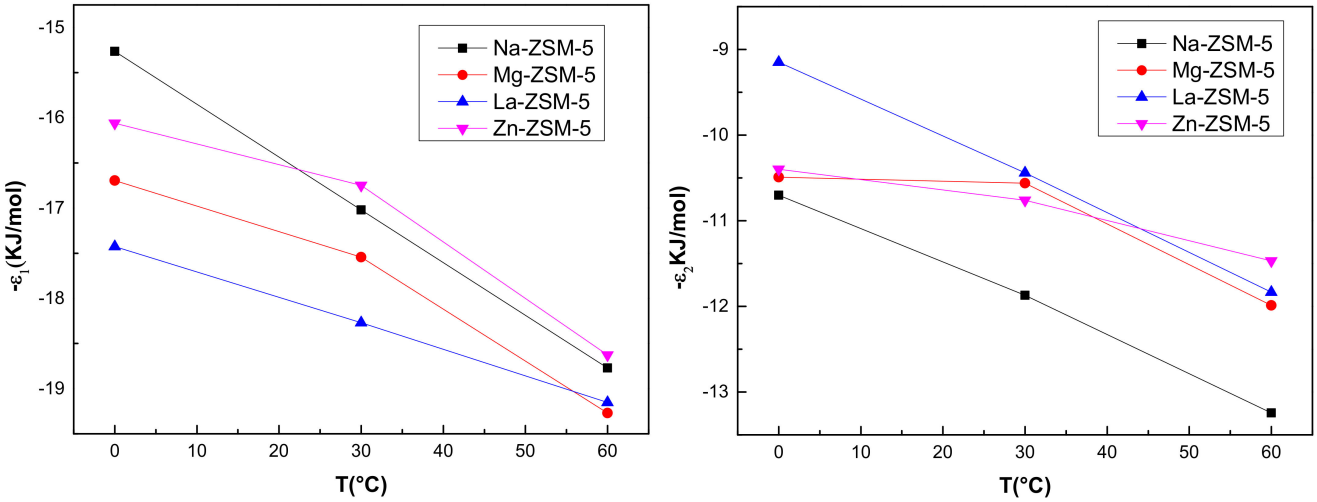

Figure 9. Effect of temperature on the CO_2 adsorption energy ($-\varepsilon_1$ and $-\varepsilon_2$) of the Na-ZSM-5, Mg-ZSM-5, La-ZSM-5 and Zn-ZSM-5 adsorbents.

7. Investigation of the Surface Adsorption Energy

Based on the adsorption energy (ε), which is related to the pressures at half saturation (P_1) and (P_2) of the substance, we determined the site energy distribution using the formalism of Polanyi potential [38,39].

$$P = P_{vs}e^{\frac{-\varepsilon}{k_B T}} \quad (7)$$

The tested isotherms $Q_a(P)$ can be described versus εand becomes $Q_a(\varepsilon)$ by incorporating Equation (7) in Equation (3). Afterwards, the site energy distribution $F(\varepsilon)$ is given by identifying the isotherms Q_a (e) versus ε.

$$F(\varepsilon) = \frac{dQ_a}{d\varepsilon} \quad (8)$$

Figure 10 presents the adsorption energy distributions (AED) determined at the three temperatures for the CO_2 adsorption on M-ZSM-5 (M= Na^+, Mg^{2+}, Zn^{2+}, La^{3+}). From this figure, we can observe that the majority of (AED) curves present two peaks. Indeed, these peaks define the equilibrium energies of the heterogeneous sites. Despite the identical shape of AED curves at different temperatures, we noticed the difference of energy distribution intensities, corresponding to the maxima peaks. The higher intensity of energy is observed for La-ZSM-5 at T = 273K, confirming the difference structure in the various tested zeolites. The increase in temperature leads to the decrement in energy distribution values explaining that the receptor sites with weak energy become fewer available for CO adsorption. The van der Waals interactions responsible for this process are confirmed by the AED values, which ranged from 10 to 25 KJ/mol for the four tested substances [35–37]. Consequently, this energy distribution interpretation confirms the type of interactions and shows that the four tested samples are characterized by a heterogeneous energy surfaces.

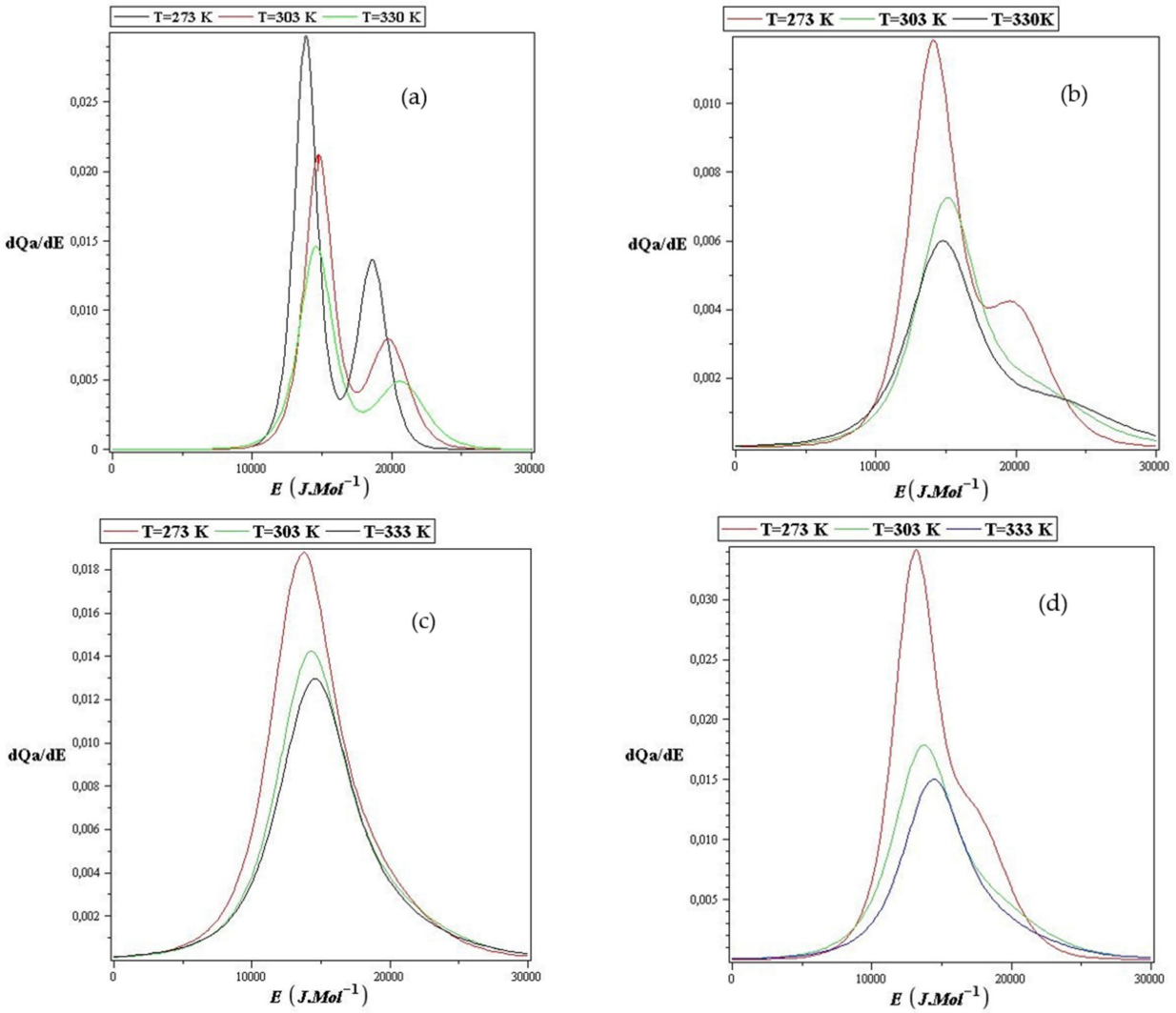

Figure 10. Site energy distributions of CO_2 adsorption onto (**a**) Na-ZSM-5, (**b**) Mg-ZSM-5, (**c**) La-ZSM-5 and (**d**) Zn-ZSM-5 at the three tested temperatures.

8. Thermodynamic Studies

In order to study the thermodynamic behavior of CO_2 adsorption on ZSM-5, certain thermodynamic functions, such as the internal energy and free energy, were determined using the multilayer model with saturation.

8.1. Gibbs Free Energy

This function allows the description of the spontaneity of the tested systems. It was obtained based on the equation as follows [39]:

$$G_a = \mu n N_0 = \mu Q_a \quad (9)$$

Figure 11 depicts the free enthalpy variation versus temperature and pressure. From the observation of this figure, we can conclude that all the G_a values are negative, explicating that the CO_2 adsorption on ZSM-5 is spontaneous. The increase in temperature leads to the decrease in this function by absolute value, showing a decrement in the feasibility of adsorption process at elevated temperatures.

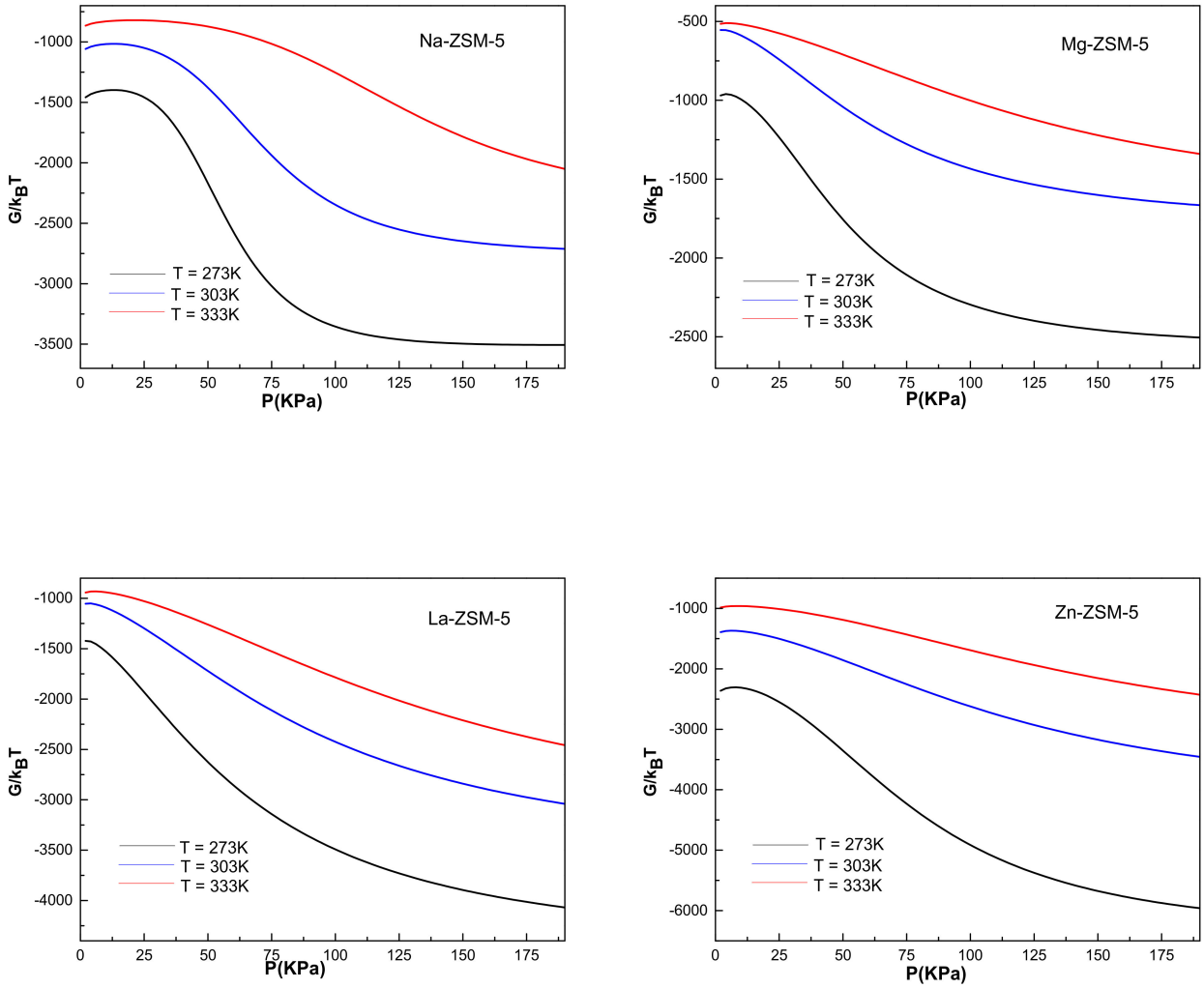

Figure 11. Evolution of Gibbs free energy versus pressure for the four tested systems at three temperatures.

8.2. Internal Energy

The internal energy (E_{int}) of the system is called the total energy that a thermodynamic system contains. It is notably due to the interactions that exist between the adsorbent and

the adsorbate. Using the analytical multilayer model with saturation, we calculated the expression of the internal energy given by [39–41]:

$$E_{int} = -\frac{\partial LnZ_{gc}}{\partial \beta} + \frac{\mu}{\beta}\left(\frac{\partial LnZ_{gc}}{\partial \mu}\right) \quad (10)$$

The internal energy variation of the four tested systems versus the pressure at three temperatures is presented in Figure 12. We can observe that all the internal energy values are less than zero, indicating the release of energy by the treated systems, which confirm the exothermic character of the adsorption mechanism [41]. In addition, we noticed the appearance of lateral interactions between CO_2 molecules on the ZSM-5 surface explained by the increase in the internal energy with the increase in the temperature.

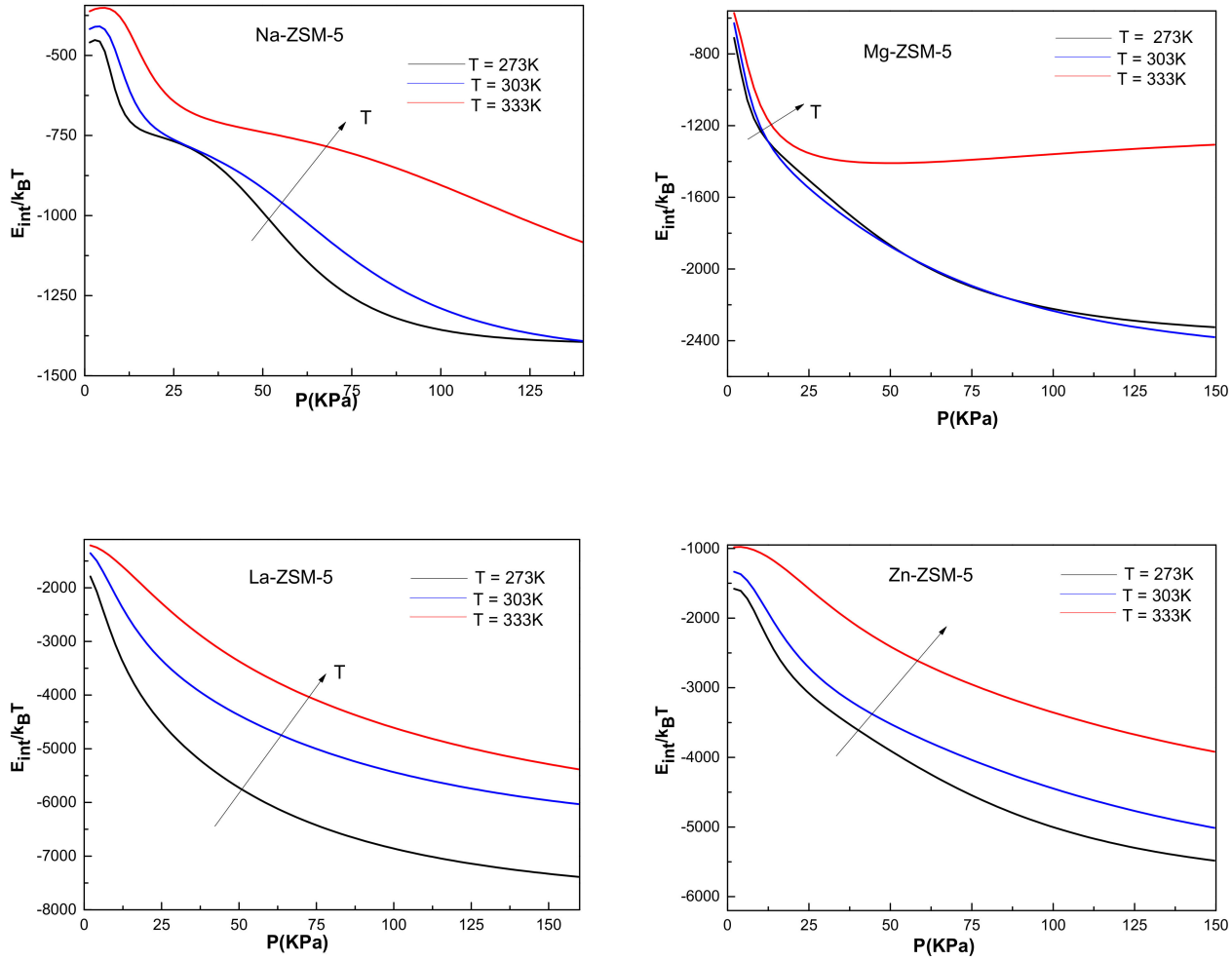

Figure 12. Evolution of internal energy versus pressure for the four tested systems at three temperatures.

9. Discussion

Taking into consideration their differing charges, sizes and chemical structures, M-ZSM-5 (M= Na^+, Mg^{2+}, Zn^{2+}, La^{3+}) were employed as adsorbents presenting their effect for the adsorption experiments (Figure 4). According to the experimental results, we can note that the CO_2 adsorption capacities of all the tested samples decrease versus temperature. The advanced multilayer model implied physicochemical parameters that play an important role on the study of the behavior of adsorption amount through the type of adsorbents and the effect of temperature. We noted that the total number of adsorbed layers (N_c) (Figure 7) and the adsorption pressure (Figure 9) raised with the temperature. However, the number of adsorbed molecules per site (n) (Figure 5), the density of receptor sites (D_m)

(Figure 6) decreased as a function of temperature. Consequently, we can conclude that total number of adsorbed layers and the adsorption pressure did not present the main factor of adsorption phenomenon. On contrary, the others parameters play a key role in explaining the exothermic character of the adsorption process. Moreover, the increment in the adsorbed quantity at saturation (Q_{sat}) with the decrement in temperature is analyzed by the exothermicity of the adsorption mechanism for the four tested systems. The steric investigation via the statistical physics model is the main factor to choose Zn-ZSM-5 zeolite as the best adsorbent for the CO_2 adsorption. Therefore, an investigation of the porosity of the different used systems would be worthwhileto see the relationship between porosity and sizes of different ions, on the one hand, and the adsorbed quantity, on the other hand, in order to optimize this relationship. Another prospect is to see the effect of an eventual role of H^+ ions in the adsorption process, i.e., to see the role of the pH in this process.

10. Conclusions

In this work, CO_2 adsorption on four adsorbents, namely M-ZSM-5 (M= Na^+, Mg^{2+}, Zn^{2+}, La^{3+}), was theoretically studied. In particular, the modeling interpretation, generally assumed for the liquid system and depending on the formalism of statistical physics, was developed and performed to analyze for the first time the measured adsorption data of CO_2 on ZSM-5. Depending on the experimental conditions, the multilayer model fitted well with the measured isotherms, giving an advanced microscopic interpretation of the adsorption process. The simulation findings indicated that the adsorption capacity of Zn-ZSM-5 is higher than that of La-ZSM-5, Na-ZSM-5 and Mg-ZSM-5; moreover, this parameter was improved with the decrease in the operating temperature. The zeolite surface and the type of cations were also controlled as well as the adsorbents performance. The adsorption energy values of adsorption were inferior to 30 kJ/mol and indicated the appearance of a physisorption process, for which the van der Waals interaction was responsible. The AED interpretation showed the physical character of adsorption mechanism. Finally, the variation of the internal energy and the Gibbs free energy versus temperature confirmed the exothermic character of the adsorption mechanism and the spontaneity of this process.

Author Contributions: Formal analysis, W.A.; Investigation, F.A. and N.K.; Methodology, N.B.; Software, Z.E.; Supervision, A.B.L. All authors have read and agreed to the published version of the manuscript.

Funding: Princess Nourah bint Abdulrahman University Researchers Supporting Project (Grant No. PNURSP2022R46), Princess Nourah bint Abdulrahman University, Riyadh, Saudi Arabia.

Institutional Review Board Statement: Not applicable.

Informed Consent Statement: Not applicable.

Data Availability Statement: Not applicable.

Acknowledgments: The authors express their gratitude to Princess Nourah bint Abdulrahman University Researchers Supporting Project (Grant No. PNURSP2022R46), Princess Nourah bint Abdulrahman University, Riyadh, Saudi Arabia.

Conflicts of Interest: The authors declare no conflict of interest.

References

1. Lee, S.C.; Kwon, Y.M.; Park, Y.H.; Lee, W.S.; Park, J.J.; Ryu, C.K.; Yi, C.K.; Kim, J.C. Structure effects of potassium-based TiO_2 sorbents on the CO_2 capture capacity. *Top Catal.* **2010**, *53*, 641–647. [CrossRef]
2. *Emissions of Greenhouse Gases in the United States*; Energy Information Administration: Washington, DC, USA, 2003.
3. Intergovernmental Panel on Climate Change (IPCC). *IPCC Special Report on Carbon Dioxide Capture and Storage*; Intergovernmental Panel on Climate Change (IPCC): Geneva, Switzerland, 2005.
4. Olajire, A.A. Recent progress on the nanoparticles-assisted greenhouse carbon dioxide conversion processes. *J. CO2 Util.* **2018**, *24*, 522–547. [CrossRef]
5. Kenarsari, S.D.; Yang, D.; Jiang, G.; Zhang, S.; Wang, J.; Russell, A.G.; Wei, Q.; Fan, M. Review of recent advances in carbon dioxide separation and capture. *RSC Adv.* **2013**, *3*, 22739–22773. [CrossRef]

6. Luis, P.; Gerven, T.V.; der Bruggen, B.V. Recent developments in membrane-based technologies for CO_2 capture. *Prog. Energy Combust. Sci.* **2012**, *38*, 419–448. [CrossRef]
7. Hedin, N.; Andersson, L.; Bergstrm, L.; Yan, J. Adsorbents for the post-combustion capture of CO_2 using rapid temperature swing or vacuum swing adsorption. *Appl. Energy* **2013**, *104*, 418–433. [CrossRef]
8. Hadri, N.E.; Quang, D.V.; Goetheer, E.L.; Zahra, M.R.A. Aqueous amine solution characterization for post-combustion CO_2 capture process. *Appl. Energy* **2017**, *185*, 1433–1449. [CrossRef]
9. Bhatta, L.K.; Subramanyam, S.; Chengala, M.D.; Bhatta, U.M.; Venkatesh, K. Enhancement in CO_2 adsorption on hydrotalcite-based material by novel carbon support combined with K_2CO_3 impregnation. *Ind. Eng. Chem. Res.* **2015**, *54*, 10876–10884. [CrossRef]
10. You, H.S.; Jin, H.; Mo, Y.H.; Park, S.E. CO_2 adsorption behavior of microwave synthesized zeolite beta. *Mater. Lett.* **2013**, *108*, 106–109. [CrossRef]
11. Chen, C.; Huang, H.; Yu, Y.; Shi, J.; He, C.; Albilali, R.; Pan, H. Template-free synthesis of hierarchical porous carbon with controlled morphology for CO_2 efficient capture. *Chem. Eng. J.* **2018**, *353*, 584–594. [CrossRef]
12. Chen, C.; Yu, Y.; He, C.; Wang, L.; Huang, H.; Albilali, R.; Cheng, J.; Hao, Z. Efficient capture of CO_2 over ordered micro-mesoporous hybrid carbon nanosphere. *Appl. Surf. Sci.* **2018**, *439*, 113–121. [CrossRef]
13. Zhao, A.; Samanta, A.; Sarkar, P.; Gupta, R. Carbon dioxide adsorption on amine impregnated mesoporous SBA-15 sorbents: Experimental and kinetics study. *Ind. Eng. Chem. Res.* **2013**, *52*, 6480–6491. [CrossRef]
14. Nelson, K.M.; Mahurin, S.M.; Mayes, R.T.; Williamson, B.; Teague, C.M.; Binder, A.J.; Baggetto, L.; Veith, G.M.; Dai, S. Preparation and CO_2 adsorption properties of softtemplated mesoporous carbons derived from chestnut tannin precursors. *Microporous Mesoporous Mater.* **2016**, *222*, 94–103. [CrossRef]
15. Ullah, R.; Saad, M.A.H.S.; Aparicio, S.; Atilhan, M. Adsorption equilibrium studies of CO2, CH4 and N2 on various modified zeolites at high pressures up to 200 bars. *Microporous Mesoporous Mater.* **2018**, *262*, 49–58. [CrossRef]
16. Zhang, C.; Wu, Q.; Lei, C.; Pan, S.; Bian, C.; Wang, L.; Meng, X.; Xiao, F.S. Solvent-free and mesoporogen-free synthesis of mesoporous aluminosilicate ZSM-5 zeolites with superior catalytic properties in the methanol-to-olefins reaction. *Ind. Eng. Chem. Res.* **2017**, *56*, 1450–1460. [CrossRef]
17. Ding, W.; Klumpp, M.; Li, H.; Schygulla, U.; Pfeifer, P.; Schwieger, W.; Haas-Santo, K.; Dittmeyer, R. Investigation of high-temperature and high-pressure gas adsorption in zeolite H-ZSM-5 via the langatate crystal microbalance: CO_2, H_2O, methanol, and dimethyl ether. *J. Phys. Chem. C* **2015**, *119*, 23478–23485. [CrossRef]
18. Weng, X.; Sun, P.; Long, Y.; Meng, Q.; Wu, Z. Catalytic oxidation of chlorobenzene over Mn_xCe_{1-x} O_2/HZSM-5 catalysts: A Study with practical implications. *Environ. Sci. Technol.* **2017**, *51*, 8057–8066. [CrossRef]
19. Sun, P.; Wang, W.; Dai, X.; Weng, X.; Wu, Z. Mechanism study on catalytic oxidation of chlorobenzene over Mn_xCe_{1-x} O_2/HZSM-5 catalysts under dry and humid conditions. *Appl. Catal. B Environ.* **2016**, *198*, 389–397. [CrossRef]
20. Pham, T.D.; Liu, Q.; Lobo, R.F. Carbon dioxide and nitrogen adsorption on cationexchanged SSZ-13 zeolites. *Langmuir* **2012**, *29*, 832–839. [CrossRef] [PubMed]
21. Zhang, J.; Singh, R.; Webley, P.A. Alkali and alkaline-earth cation exchanged chabazite zeolites for adsorption based CO_2 capture. *Microporous Mesoporous Mater.* **2008**, *11*, 478–487. [CrossRef]
22. Walton, K.S.; Abney, M.B.; Douglas LeVan, M. CO_2 adsorption in Y and X zeolites modified by alkali metal cation exchange. *Microporous Mesoporous Mater.* **2006**, *91*, 78–84. [CrossRef]
23. Li, Z.; Sellaoui, L.; Dotto, G.L.; Bonilla-Petriciolet, A.; Lamine, B.A. Understanding theadsorption mechanism of phenol and 2-nitrophenol on a biopolymer-based biochar in single and binary systems via advanced modeling analysis. *Chem. Eng.* **2019**, *371*, 1–6. [CrossRef]
24. Sellaoui, L.; Dotto, G.L.; Peres, E.C.; Benguerba, Y.; Lima, E.C.; Lamine, A.B.; Erto, A. New insights into the adsorption of Crystal Violet dye on functionalized multiwalled carbon nanotubes: Experiments, statistical physics and COSMO–RS models application. *J. Mol. Liq.* **2017**, *248*, 890–897. [CrossRef]
25. Wang, Y.; Du, T.; Jia, H.; Qiu, Z.; Song, Y. Effect of extra-framework cation in ion-exchanged ZSM-5 from rice husk ash on CO_2 adsorption. *Solid State Sci.* **2019**, *97*, 105985. [CrossRef]
26. Zhang, L.; Sellaoui, L.; Franco, D.; Dotto, G.L.; Bajahzar, A.; Belmabrouk, H.; Bonilla-Petriciolet, A.; Oliveira, M.L.S.; Lia, Z. Adsorption of dyes brilliant blue, sunset yellow and tartrazine from aqueous solution on chitosan: Analytical interpretation via multilayer statistical physics model. *Chem. Eng. J.* **2020**, *382*, 122952. [CrossRef]
27. Li, Z.; Dotto, G.L.; Bajahzar, A.; Sellaoui, L.; Belmabrouk, H.; Ben Lamine, A.; Bonilla-Petriciolet, A. Adsorption of indium (III) from aqueous solution on raw, ultrasound- and supercritical-modified chitin: Experimental and theoretical analysis. *Chem. Eng. J.* **2019**, *373*, 1247–1253. [CrossRef]
28. Pang, X.; Sellaoui, L.; Franco, D.; Netto, M.S.; Georgin, J.; Dotto, G.L.; Abu Shayeb, M.K.; Belmabrouk, H.; Bonilla-Petriciolet, A.; Li, Z. Preparation and characterization of a novel mountain soursop seeds powder adsorbent and its application for the removal of crystal violet and methylene blue from aqueous solutions. *Chem. Eng. J.* **2020**, *391*, 123617. [CrossRef]
29. Hemalatha, P.; Bhagiyalakshmi, M.; Ganesh, M.; Palanichamy, M.; Murugesan, V.; Jang, H.T. Role of ceria in CO_2 adsorption on NaZSM-5 synthesized using rice husk ash. *J. Ind. Eng. Chem.* **2012**, *18*, 260–265. [CrossRef]
30. Westermann, A.; Azambre, B.; Bacariza, M.; Graça, I.; Ribeiro, M.; Lopes, J.; Henriques, C. The promoting effect of Ce in the CO_2 methanation performances on NiUSY zeolite: A FTIR in Situ/Operando study. *Catal. Today* **2017**, *83*, 74–81. [CrossRef]

31. Yang, S.T.; Kim, J.; Ahn, W.S. CO_2 adsorption over ion-exchanged zeolite beta with alkali and alkaline earth metal ions. *Microporous Mesoporous Mater.* **2010**, *135*, 90–94. [CrossRef]
32. Du, T.; Che, S.; Liu, L.; Fang, X. Preparation of zinc chabazite (ZnCHA) for CO_2capture. *Res. Chem. Intermed.* **2017**, *43*, 1783–1792. [CrossRef]
33. Al-Yousef, H.; Alotaibi, M.B.; Alanazi, M.M.; Aouaini, F.; Sellaoui, L.; Bonilla-Petriciolet, A. Theoretical assessment of the adsorption mechanism of ibuprofen, ampicillin, orange G and malachite green on a biomass functionalized with plasma. *J. Environ. Chem. Eng.* **2021**, *9*, 104950. [CrossRef]
34. Bouaziz, N.; Aouaini, F.; Ben Torkia, Y.; Altowyan, S.A.; Ben Lamine, A. Advanced interpretation of hydrogen absorption process in LaMgNi3.6M0.4 (M = Ni, Mn, Al, Co, Cu) alloys using statistical physics treatment. *Int. J. Hydrogen Energy* **2021**, *6*, 10389–10395. [CrossRef]
35. Aouaini, F.; Bouazizi, N.; Almoneef, M.M.; Al-Ghamdi, H.; Ben Lamine, A. Absorption and desorption of hydrogen in Ti1.02Cr1.1Mn0.3Fe0.6RE0.03: Experiments characterization and analytical interpretation using statistical physics treatment. *RSC Adv.* **2021**, *11*, 15905. [CrossRef]
36. Aouaini, F. Water vapor molecule adsorption onto 'Ajwa' dates: Analytical investigation via infinite multilayer statistical physics model. *Arab. J. Chem.* **2021**, *14*, 103248. [CrossRef]
37. Bouaziz, N.; Bouzid, M.; Ben Lamine, A. Theoretical study of hydrogen absorption and desorption in $Ti_{1-x}Zr_xMn_{1.4}$ using statistical physics treatment: Microscopic investigation and thermodynamic potential interpretation. *Int. J. Hydrogen Energy* **2018**, *43*, 1615–1633. [CrossRef]
38. Wjihi, S.; Yang, J.; Sellaoui, L.; Knani, S.; Ben Lamine, A. Interpreting the hydrogen adsorption on organic groups functionalized MOF-5s by statistical physics model. *Int. J. Hydrogen Energy* **2017**, *42*, 10023–10037. [CrossRef]
39. Kumar, K.V.; Castro, M.M.; Martinez-Escandell, M.; Molina-Sabio, M.; Silvestre-Albero, J.; Rodriguez-Reinoso, F. A continuous site energy distribution function from Redlich-Peterson isotherm for adsorption on heterogeneous surfaces. *Chem. Phys. Lett.* **2010**, *492*, 187–192. [CrossRef]
40. Carter, M.C.; Kilduff, J.E.; Weber, W.J., Jr. Site energy distribution analysis of preloaded adsorbents. *Environ. Sci. Technol.* **1995**, *29*, 1773–1780. [CrossRef]
41. Diu, B.; Guthmann, C.; Lederer, D.; Roulet, B. Macroscopic motion of a totally isolated system in statistical equilibrium. *Am. J. Phys.* **1990**, *58*, 974–978. [CrossRef]